Data-Efficient Model Learning for Control with Jacobian-Regularized Dynamic Mode Decomposition

Anonymous Author(s)
Affiliation
Address
email

Abstract: We present a novel algorithm for learning Koopman models of controlled nonlinear dynamical systems from data based on Dynamic-Mode Decomposition (DMD). Our approach, Jacobian-Regularized DMD (JDMD), offers dramatically improved sample efficiency over existing DMD-based algorithms by leveraging Jacobian information from an approximate prior model of the system. We demonstrate JDMD's ability to quickly learn bilinear Koopman dynamics representations across several realistic examples in simulation, including a quadrotor and a perching fixed-wing aircraft. In all cases, we show that the models learned by JDMD provide superior tracking and generalization performance in a model-predictive control framework when compared to both the approximate prior models used in training and models learned by standard extended DMD.

1 Introduction

In recent years, both model-based optimal-control [1, 2, 3, 4] and data-driven reinforcement-learning methods [5, 6, 7] have demonstrated impressive successes on complex, nonlinear robotic systems. However, both of approaches suffer from inherent drawbacks: Data-driven methods often require extremely large amounts of data and fail to generalize outside of the domain or task on which they were trained. On the other hand, model-based methods require an accurate model of the system to achieve good performance. In many cases, high-fidelity models can be too difficult to construct from first principles or too computationally expensive to be of practical use. However, low-order approximate models that can be evaluated cheaply at the expense of controller performance are often available. With this in mind, we seek a middle ground between model-based and data-driven approaches in this work.

We propose a method for learning bilinear Koopman models of nonlinear dynamical systems for use in model-predictive control that leverages information from an approximate prior dynamics model of the system in the training process. Our new algorithm builds on extended Dynamic Mode Decomposition (EDMD), which learns Koopman models from trajectory data [8, 9, 10, 11, 12], by adding a derivative regularization term based on derivatives computed from a prior model. We show that this new algorithm, Jacobian-regularized Dynamic Mode Decomposition (JDMD), can learn models with dramatically fewer samples than EDMD, even when the prior model differs significantly from the true dynamics of the system. We also demonstrate the effectiveness of these learned models in a model-predictive control (MPC) framework. The result is a fast, robust, and sample-efficient pipeline for quickly training a model that can outperform previous Koopman-based MPC approaches as well as purely model-based controllers that do not leverage data collected from the actual system.

Our work is most closely related to the recent work of Folkestad et. al. [11, 13, 14], which learn bilinear models and apply nonlinear model-predictive control directly on the learned bilinear dynamics. Other recent works have combined linear Koopman models with model-predictive control [10] and Lyapunov control techniques with bilinear Koopman [15]. Our contributions are:

Submitted to the 6th Conference on Robot Learning (CoRL 2022). Do not distribute.

- A novel extension to extended dynamic mode decomposition, called JDMD, that incorporates gradient information from an approximate analytic model
- A recursive, batch QR algorithm for solving the least-squares problems that arise when learning bilinear dynamical systems using DMD-based algorithms, including JDMD and EDMD
- A simple linear MPC control technique for learned bilinear control systems that is computationally efficient and, when combined with JDMD, requires very little training data to achieve good performance

The remainder of the paper is organized as follows: In Section 2 we provide some background on the application of Koopman operator theory to controlled dynamical systems and review some related works. Section 3 then describes the proposed JDMD algorithm. In Section 4 we outline a memory-efficient technique for solving the large, sparse linear least-squares problems that arise when applying JDMD and other DMD-based algorithms. Next, in Section 5, we propose an efficient model-predictive control technique that utilizes the learned bilinear models produced by JDMD. Section 6 then provides simulation results and analysis of the proposed algorithm applied to control tasks on a cartpole, a quadrotor, and a small foam airplane, all subject to significant model mismatch. In Section 7 we discuss the limitations of our approach, followed by some concluding remarks in Section 8.

2 Background and Related Work

2.1 Koopman Operator Theory

The theoretical underpinnings of the Koopman operator and its application to dynamical systems has been extensively studied [16, 17, 9, 18]. Rather than describe the theory in detail, we highlight the key concepts employed by the current work and refer the reader to the existing literature on Koopman theory for further details.

We start by assuming a controlled, nonlinear, discrete-time dynamical system,

$$x^+ = f(x, u), \tag{1}$$

where $x \in \mathcal{X} \subseteq \mathbb{R}^{N_x}$ is the state vector, $u_k \in \mathbb{R}^{N_u}$ is the control vector, and x^+ is the state at the next time step. The key idea behind the Koopman operator is that the nonlinear finite-dimensional dynamics (1) can be represented *exactly* by an infinite-dimensional bilinear system of the form,

$$y^+ = Ay + Bu + \sum_{i=1}^{m} u_i C_i y = g(y, u), \tag{2}$$

where $y = \phi(x)$ is a nonlinear mapping from the finite-dimensional state space $\mathcal{X}$ to the infinite-dimensional Hilbert space of *observables* $\mathcal{Y}$. In practice, we approximate (2) by restricting $\mathcal{Y}$ to be a finite-dimensional vector space, in which case ϕ becomes a finite-dimensional nonlinear function of the state variables that must be chosen by the user.

Intuitively, ϕ "lifts" our state x into a higher dimensional space $\mathcal{Y}$ where the dynamics are approximately (bi)linear, effectively trading dimensionality for (bi)linearity. Similarly, we can perform the inverse operation by projecting a lifted state y back into the original state space $\mathcal{X}$. In this work, we will assume that ϕ is constructed in such a way that this inverse mapping is linear:

$$x = Gy \tag{3}$$

2.2 Extended Dynamic Mode Decomposition

A lifted bilinear system of the form (2) can be learned from P samples of the system dynamics (x_j^+, x_j, u_j) using Extended Dynamic Mode Decomposition (EDMD) [18, 13]. We first define the

following data matrices:

$$Z_{1:P} = \begin{bmatrix} y_1 & y_2 & \dots & y_P \\ u_1 & u_2 & \dots & u_P \\ u_{1,1}y_1 & u_{2,1}y_2 & \dots & u_{P,1}y_P \\ \vdots & \vdots & \ddots & \vdots \\ u_{1,m}y_1 & u_{2,m}y_2 & \dots & u_{P,m}y_P \end{bmatrix}, \quad Y^+_{1:P} = \begin{bmatrix} y_1^+ & y_2^+ & \dots & y_P^+ \end{bmatrix}, \tag{4}$$

We then concatenate all of the model coefficient matrices as follows:

$$E = [A \quad B \quad C_1 \quad \dots \quad C_m] \in \mathbb{R}^{N_y \times N_z}, \tag{5}$$

The model learning problem can then be written as the following linear least-squares problem:

$$\underset{E}{\text{minimize}} \left\| EZ_{1:P} - Y^+_{1:P} \right\|_2^2 \tag{6}$$

3 Jacobian-Regularizated Dynamic Mode Decomposition

We now present JDMD as a straightforward adaptation of the original EDMD algorithm described in Section 2.2. Given P samples of the dynamics (x_i^+, x_i, u_i), and an approximate discrete-time dynamics model,

$$x^+ = \tilde{f}(x, u), \tag{7}$$

we can evaluate the Jacobians of our approximate model $\tilde{f}$ at each of the sample points: $\tilde{A}_i = \frac{\partial \tilde{f}}{\partial x}, \tilde{B}_i = \frac{\partial \tilde{f}}{\partial u}$. After choosing a nonlinear mapping $\phi : \mathbb{R}^{N_x} \mapsto \mathbb{R}^{N_y}$ our goal is to find a bilinear dynamics model (2) that matches the Jacobians of our approximate model, while also matching our dynamics samples. We accomplish this by penalizing differences between the Jacobians of our learned bilinear model with respect to the original states x and controls u, and the Jacobians we expect from our analytical model. These *projected Jacobians* are calculated by differentiating through the *projected dynamics*:

$$x^+ = G\left(A\phi(x) + Bu + \sum_{i=1}^{m} u_i C_i \phi(x)\right) = \bar{f}(x, u). \tag{8}$$

Differentiating (8) with respect to x and u gives us

$$\bar{A}_j = \frac{\partial \hat{f}}{\partial x}(x_j, u_j) = G\left(A + \sum_{i=1}^{m} u_{j,i} C_i\right)\Phi(x_j) = GE\hat{A}(x_j, u_j) = GE\hat{A}_j \tag{9a}$$

$$\bar{B}_j = \frac{\partial \hat{f}}{\partial u}(x_j, u_j) = G\Big(B + [C_1 x_j \quad \dots \quad C_m x_j]\Big) = GE\hat{B}(x_j, u_j) = GE\hat{B}_j \tag{9b}$$

where $\Phi(x) = \partial\phi/\partial x$ is the Jacobian of the nonlinear map ϕ, and

$$\hat{A}(x, u) = \begin{bmatrix} I_{N_y} \\ 0 \\ u_1 I_{N_y} \\ u_2 I_{N_y} \\ \vdots \\ u_m I_{N_y} \end{bmatrix} \Phi(x) \in \mathbb{R}^{N_z \times N_x}, \quad \hat{B}(x, u) = \begin{bmatrix} 0 \\ I_{N_u} \\ [x\ 0\ \dots\ 0] \\ [0\ x\ \dots\ 0] \\ \vdots \\ [0\ 0\ \dots\ x] \end{bmatrix} \in \mathbb{R}^{N_z \times N_u}. \tag{10}$$

We then solve the following linear least-squares problem:

$$\underset{E}{\text{minimize}} \ \ (1-\alpha)\left\| EZ_{1:P} - Y^+_{1:P} \right\|_2^2 + \alpha \sum_{j=1}^{P} \left(\left\| GE\hat{A}_j - \tilde{A}_j \right\|_2^2 + \left\| GE\hat{B}_j - \tilde{B}_j \right\|_2^2 \right) \tag{11}$$

The resulting linear least-squares problem has $(N_y + N_x^2 + N_x \cdot N_u) \cdot P$ rows and $N_y \cdot N_z$ columns. Given that the number of rows in this problem grows quadratically with the state dimension, solving

Figure 1: Airplane perching trajectory, a high angle-of-attack maneuver that minimizes velocity at the goal position

this problem can be challenging from a computational perspective. In the Section 4, we propose an algorithm for solving these problems without needing to move to a distributed-memory setup in order to solve these large linear systems. The proposed method also provides a straightforward way to approach incremental updates to the bilinear system, where the coefficients could be efficiently learned "live" while the robot gathers data by moving through its environment.

4 Efficient Recursive Least Squares

In its canonical formulation, a linear least squares problem can be represented as the following unconstrained optimization problem:

$$\min_x \|Fx - d\|_2^2. \tag{12}$$

We assume F is a large, sparse matrix and that solving it directly using a QR or Cholesky decomposition requires too much memory for a single computer. While solving (12) using an iterative method such as LSMR [19] or LSQR [20] is possible, we find that these methods do not work well in practice for solving (11) due to ill-conditioning. Standard recursive methods for solving these problems are able to process the rows of the matrices sequentially to build a QR decomposition of the full matrix, but also tend to suffer from ill-conditioning [21, 22, 23].

To overcome these issues, we propose an alternative recursive method based. We solve (12) by dividing up rows of F into batches:

$$F^T F = F_1^T F_1 + F_2^T F_2 + \ldots + F_N^T F_N. \tag{13}$$

The main idea is to maintain and update an upper-triangular Cholesky factor U_i of the first i terms of the sum (13). Given U_i, we can calculate U_{i+1} using the QR decomposition, as shown in [24]:

$$U_{i+1} = \sqrt{U_i^T U_i + F_{i+1}^T F_{i+1}} = \mathrm{QR_R}\left(\begin{bmatrix} U_i \\ F_{i+1} \end{bmatrix}\right), \tag{14}$$

where $\mathrm{QR_R}$ returns the upper triangular matrix R from the QR decomposition. For an efficient implementation, this function should be an "economy" or "Q-less" QR decomposition since the Q matrix is never needed.

We also handle regularization of the normal equations, equivalent to adding Tikhonov regularization to the original least squares problem, during the base case of our recursion. If we want to add an L2 regularization with weight λ, we calculate U_1 as:

$$U_1 = \mathrm{QR_R}\left(\begin{bmatrix} F_1 \\ \sqrt{\lambda} I \end{bmatrix}.\right). \tag{15}$$

5 Projected Bilinear MPC

We propose a simple approach to model-predictive control for the bilinear systems learned using either classic EDMD or the proposed JDMD approach. The key idea is to use the projected Jacobians $\bar{A}$ and $\bar{B}$ in (9), effectively reducing the problem to a standard linear MPC problem in the original

state space instead of the larger, lifted one. In the all of the examples in the following section, our MPC controller solves the following convex Quadratic Program (QP):

$$\begin{aligned} \underset{x_{1:N},\, u_{1:N-1}}{\text{minimize}} \quad & \frac{1}{2} x_N^T Q_N x_N + \frac{1}{2} \sum_{k=1}^{N-1} x_k^T Q_k x_k + u_k^T R_k u_k \\ \text{subject to} \quad & x_{k+1} = \bar{A}_k x_k + \bar{B}_k u_k + d_k, \\ & x_1 = x_{\text{init}} \end{aligned} \tag{16}$$

where here we define x and u to be the "delta" from the reference trajectory $\bar{x}_{1:N}$, $\bar{u}_{1:N-1}$. The affine dynamics term $d_k = f(\bar{x}_k, \bar{u}_k) - \bar{x}_{k+1}$ allows for dynamically infeasible reference trajectories. The projected Jacobians can be efficiently calculated from the bilinear dynamics either offline or online, and since the problem dimension is the same size as the linear MPC problem for the original dynamics, it is no more expensive to compute. This formulation also makes it trivial to enforce additional control or path constraints, and avoids the need to regularize or otherwise constrain the lifted states.

6 Experimental Results

This section presents the results of several simulation experiments to evaluate the performance of JDMD. For each simulated system we specify two models: a *nominal* model, which is simplified and contains both parametric and non-parametric model error, and a *true* model, which is used exclusively for simulating the system and evaluating algorithm performance.

All models were trained by simulating the "true" system with a nominal controller to collect data in the region of the state space relevant to the task. A set of fixed-length trajectories were collected, each at a sample rate of 20-25 Hz. The bilinear EDMD model was trained using the same approach introduced by Folkestad and Burdick [13]. All continuous dynamics were discretized with an explicit fourth-order Runge Kutta integrator. Code for all experiments is available at TODO: removed for anonymous review.

6.1 Systems and Tasks

Cartpole: We perform a swing-up task on a cartpole system. The *true* model includes Coulomb friction between the cart and the floor, viscous damping at both joints, and a deadband in the control input that were not included in the *nominal* model. Additionally, the mass of the cart and pole model were altered by 20% and 25% with respect to the nominal model, respectively. The following nonlinear mapping was used when learning the bilinear models: $\phi(x) = [\,1,\, x,\, \sin(x),\, \cos(x),\, \sin(2x),\, \sin(4x),\, T_2(x),\, T_3(x),\, T_4(x)\,] \in \mathbb{R}^{33}$, where $T_i(x)$ is a Chebyshev polynomial of the first kind of order i. All reference trajectories for the swing up task were generated using ALTRO [24, 25].

Quadrotor: We attempt to track point-to-point linear reference trajectories from various initial conditions on both planar and full 3D quadrotor models. For both systems, the *true* model includes aerodynamic drag terms not included in the *nominal* model, as well as parametric error of roughly 5% on the system parameters (e.g. mass, rotor arm length, etc.). The planar model was trained using a nonlinear mapping of $\phi(x) = [\,1,\, x,\, \sin(x),\, \cos(x),\, \sin(2x),\, T_2(x)] \in \mathbb{R}^{25}$ while the full quadrotor model was train using a nonlinear mapping of $\phi(x) = [\,1,\, x,\, T_2(x),\, \sin(p),\, \cos(p),\, R^T v,\, v^T R R^T v,\, p \times v,\, p \times \omega,\, \omega \times \omega] \in \mathbb{R}^{44}$, where p is the quadrotor's position, v and ω are the translational and angular velocities respectively, and R is the rotation matrix.

Airplane: We perform a post-stall perching maneuver on a high-fidelity model of an airplane constructed from wind-tunnel data [26]. A demonstration perching trajectory was produced using trajectory optimization (see Figure 1) and then tracked using MPC. The nominal model uses a simple flat-plate wing model with linear lift and quadratic drag coefficient approximations. The bilinear

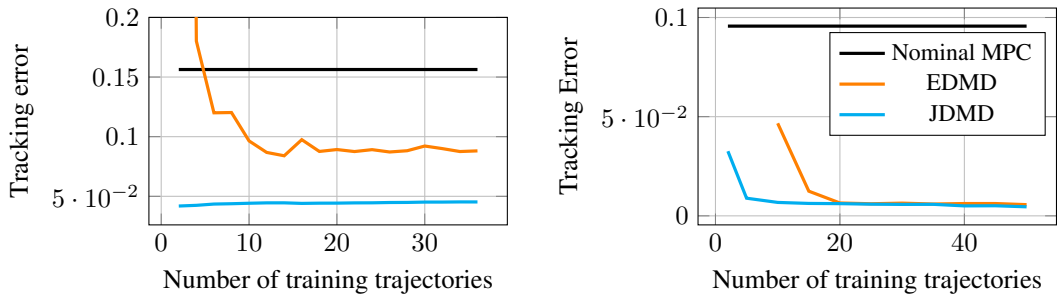

(a) Cartpole

(b) Airplane

Figure 2: MPC tracking error vs training trajectories for both the cartpole (left) and airplane (right). Tracking error is defined as the average L2 error over all the test trajectories between the reference and simulated trajectories.

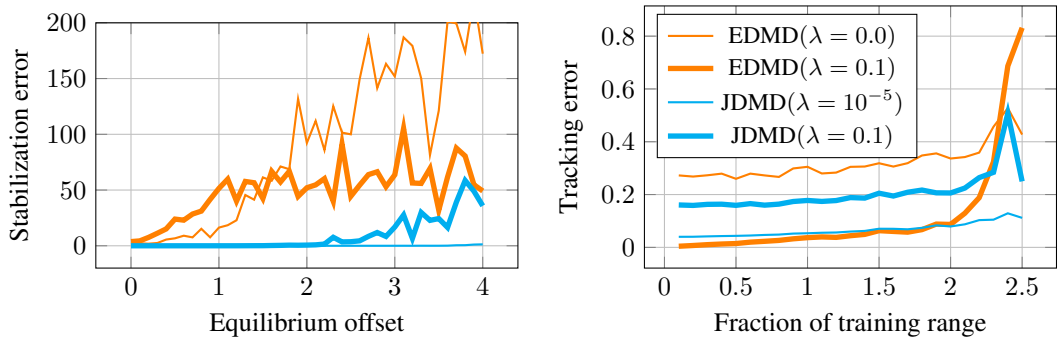

(a) LQR stabilization error over increasing equilibrium offset

(b) Tracking error for the quadrotor MPC reference trajectory tracking task.

Figure 3: Generalizability with respect to initial conditions sampled outside of the training domain. The initial conditions are sampled from a uniform distribution, whose limits are determined by a scaling of the limits used for the training distribution. A training range fraction greater than 1 indicates the distribution range is beyond that used to generate the training trajectories. The thick lines represent the algorithm with a heavy regularization parameter.

models use a 68-dimensional nonlinear mapping ϕ including terms such as the rotation matrix (expressed in terms of a Modified Rodriguez Parameter), powers of the angle of attack and side slip angle, the body frame velocity, various cross products with the angular velocity, and some 3rd and 4th order Chebyshev polynomials of the states.

6.2 Sample Efficiency

We highlight the sample efficiency of the proposed algorithm in Figure 2. For both the cartpole swing up and the airplane perch trajectory tracking tasks, the proposed method achieves better tracking than the nominal MPC controller with just two sample trajectories, and performs better than EDMD on both trajectory tracking tasks. To achieve comparable performance on the perching task, EDMD requires about 4x the number of samples (20 vs 5) compared to the proposed approach.

6.3 Generalization

We demonstrate the generalizability of the proposed method on both the planar and 3D quadrotor. In all tasks, the goal is to return to the origin, given an initial condition sampled from some uniform distribution centered at the

	Nominal	**EDMD**	**JDMD**
Tracking Err.	0.30	0.63	**0.11**
Success Rate	**82%**	18%	80%

Table 1: Performance summary of MPC tracking of 6-DOF quadrotor

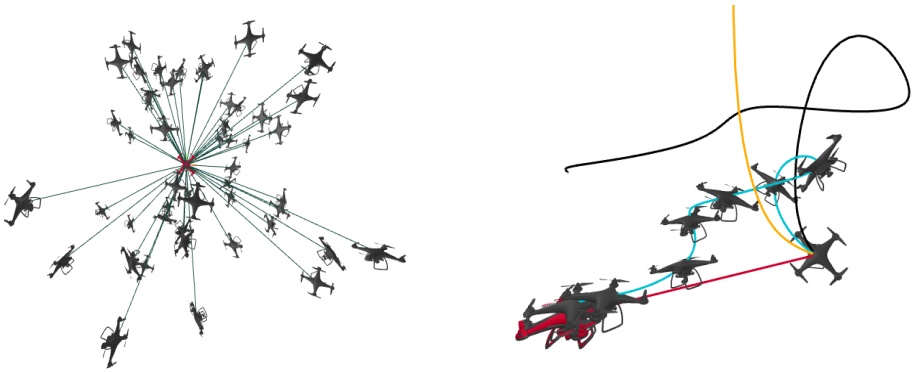

(a) Generated point-to-point trajectories and initial conditions for testing tracking MPC of 6-DOF quadrotor.

(b) Generated MPC trajectories for nominal MPC (black), EDMD (orange), and JDMD (cyan) for tracking infeasible, point-to-point trajectory (red).

Figure 4: Generalizability with respect to initial conditions sampled outside of the training domain. The initial conditions are sampled from a uniform distribution, whose limits are determined by a scaling of the limits used for the training distribution. A training range fraction greater than 1 indicates the distribution range is beyond that used to generate the training trajectories. The thick lines represent the algorithm with a heavy regularization parameter.

origin. To test the generalizability of the algorithms, we scale the size of the sampling "window" relative to the window on which it was trained, e.g. if the initial lateral position was trained on data in the interval $[-1.5, +1.5]$, we sampled the test initial condition from the window $[-\gamma 1.5, +\gamma 1.5]$. The results for the planar quadrotor are shown in Figure 3b. With a well-picked regularization value, JDMD generalized past where the performance of EDMD suffers. Additionally, in Figure 3a we show the effect of changing the equilibrium position away from the origin: while the true dynamics should be invariant to this change, EDMD fails to learn this whereas JDMD does.

For the full quadrotor, given the goal of tracking a straight line back to the origin, we test 50 initial conditions, many of which are far from the goal, have large velocities, or are nearly inverted (see Figure 4a). The results using an MPC controller are shown in Table 1, demonstrating the excellent generalizability of the algorithm, given that the algorithm was only trained on 30 initial conditions, sampled relatively sparsely given the size of the sampling window. EDMD only successfully brings about 18% of the samples to the origin, while the majority of the time resulting in trajectories like those in Figure 4b.

6.4 Lifted versus Projected MPC

We performed a simple experiment to highlight the value of the proposed "projected" MPC, outlined in Section 5. We trained EDMD and JDMD models with an increasing number of training trajectories, and recorded the first sample size at which the "lifted" and "projected" MPC controllers consistently stabilized the system (i.e. stabilized 95% of the test initial conditions for the cartpole system for that sample size and subsequent ones). The results are summarized in Table 2. The results quantitatively show what we qualitatively observed while training and testing these various examples: the projected MPC approach usually required far fewer samples to "train" and usually had better performance than its lifted counterpart that used the bilinear lifted dynamics. This was especially pronounced when combined with the proposed JDMD approach, which makes sense given that the approach explicitly encourages these Jacobians to match the analytical ones, so quickly converges to reasonable values with just a few training examples.

Friction (μ)	0.0	0.1	0.2	0.3	0.4	0.5	0.6
Nominal	✓	✓	✗	✗	✗	✗	✗
EDMD	3	19	6	14	✗	✗	✗
JDMD	2	2	2	2	3	7	12

Table 3: Training trajectories required to stabilize the cartpole with the given friction coefficient

6.5 Sensitivity to Model Mismatch

MPC	EDMD	JDMD
Lifted	17	15
Projected	18	**2**

Table 2: Training trajectories required to beat nominal MPC

While we've introduced a significant mount of model mismatch in all of the examples so far, a natural argument against model-based methods is that they're only as good as your model is at capturing the salient dynamics of the system. We investigated the effect of increasing model mismatch by incrementally increasing the Coulomb friction coefficient between the cart and the floor for the cartpole stabilization task (recall the nominal model assumed zero friction). The results are shown in Table 3. As expected, the number of training trajectories required to find a good stabilizing controller increases for the proposed approach. We achieved the results above by setting $\alpha = 0.01$, corresponding to a decreased confidence in our model, thereby placing greater weight on the experimental data. The standard EDMD approach always required more samples, and was unable to find a good enough model above friction values of 0.4. While this could likely be remedied by adjusting the nonlinear mapping ϕ, the proposed approach works well with the given bases. Note that the nominal MPC controller failed to stabilize the system above friction values of 0.1, so again, we demonstrate that we can improve MPC performance substantially with just a few training samples by combining analytical gradient information and data sampled from the true dynamics.

7 Limitations

As with most data-driven techniques, it is difficult to claim that our method will increase performance in all cases. It is possible that having an extremely poor prior model may hurt rather than help the training process. However, we found that even when the α parameter is extremely small (placing little weight on the Jacobians during the learning process), it still dramatically improves the sample efficiency over standard EDMD. It is also quite possible that the performance gaps between EDMD and JDMD shown here can be reduced through better selection of basis functions and better training data sets; however, given that the proposed approach converges to EDMD as $\alpha \to 0$, we see no reason to not adopt the proposed methodology as simply tune α based on the confidence of the model and the quantity (and quality) of training data.

8 Conclusions and Future Work

We have presented JDMD, a simple but powerful extension to EDMD that incorporates derivative information from an approximate prior model. We have tested JDMD in combination with a simple linear MPC control policy across a range of systems and tasks, and have found that the resulting combination can dramatically increase sample efficiency over EDMD, often improving over a nominal MPC policy with just a few sample trajectories. Substantial areas for future work remain: most notably, demonstrating the proposed pipeline on hardware. Additional directions include lifelong learning or adaptive control applications, combining simulated and real data through the use of modern differentiable physics engines [27, 28], residual dynamics learning, as well as the development of specialized numerical methods for solving nonlinear optimal control problems using the learned bilinear dynamics.

References

[1] F. Farshidian, M. Neunert, A. W. Winkler, G. Rey, and J. Buchli. An efficient optimal planning and control framework for quadrupedal locomotion. In *2017 {IEEE} International Conference on Robotics and Automation ({ICRA})*, pages 93–100. doi:10.1109/ICRA.2017.7989016.

[2] S. Kuindersma, F. Permenter, and R. Tedrake. An efficiently solvable quadratic program for stabilizing dynamic locomotion. pages 2589–2594. ISSN 9781479936854. doi:10.1109/ICRA.2014.6907230.

[3] M. Bjelonic, R. Grandia, O. Harley, C. Galliard, S. Zimmermann, and M. Hutter. Whole-Body MPC and Online Gait Sequence Generation for Wheeled-Legged Robots. pages 8388–8395. ISSN 9781665417143. doi:10.1109/IROS51168.2021.9636371.

[4] J. K. Subosits and J. C. Gerdes. From the racetrack to the road: Real-time trajectory replanning for autonomous driving. 4(2):309–320. doi:10.1109/TIV.2019.2904390.

[5] N. Karnchanachari, M. I. Valls, S. David Hoeller, and M. Hutter. Practical Reinforcement Learning For MPC: Learning from sparse objectives in under an hour on a real robot. pages 1–14. doi:10.3929/ETHZ-B-000404690. URL https://doi.org/10.3929/ethz-b-000404690.

[6] D. . Hoeller, F. . Farshidian, M. Hutter, F. Farshidian, and D. Hoeller. Deep Value Model Predictive Control. 100:990–1004. doi:10.3929/ETHZ-B-000368961. URL https://doi.org/10.3929/ethz-b-000368961.

[7] Z. Li, X. Cheng, X. B. Peng, P. Abbeel, S. Levine, G. Berseth, and K. Sreenath. Reinforcement Learning for Robust Parameterized Locomotion Control of Bipedal Robots. 2021-May:2811–2817. ISSN 9781728190778. doi:10.1109/ICRA48506.2021.9560769.

[8] A. Meduri, P. Shah, J. Viereck, M. Khadiv, I. Havoutis, and L. Righetti. BiConMP: A Nonlinear Model Predictive Control Framework for Whole Body Motion Planning. doi:10.48550/arxiv.2201.07601. URL https://arxiv.org/abs/2201.07601v1.

[9] D. Bruder, X. Fu, and R. Vasudevan. Advantages of Bilinear Koopman Realizations for the Modeling and Control of Systems with Unknown Dynamics. 6(3):4369–4376. doi:10.1109/LRA.2021.3068117.

[10] M. Korda and I. Mezić. Linear predictors for nonlinear dynamical systems: Koopman operator meets model predictive control. 93:149–160. doi:10.1016/j.automatica.2018.03.046. URL https://doi.org/10.1016/j.automatica.2018.03.046.

[11] C. Folkestad, D. Pastor, and J. W. Burdick. Episodic Koopman Learning of Nonlinear Robot Dynamics with Application to Fast Multirotor Landing. pages 9216–9222. ISSN 9781728173955. doi:10.1109/ICRA40945.2020.9197510.

[12] H. J. Suh and R. Tedrake. The Surprising Effectiveness of Linear Models for Visual Foresight in Object Pile Manipulation. 17:347–363. doi:10.48550/arxiv.2002.09093. URL https://arxiv.org/abs/2002.09093v3.

[13] C. Folkestad and J. W. Burdick. Koopman NMPC: Koopman-based Learning and Nonlinear Model Predictive Control of Control-affine Systems. In *Proceedings - IEEE International Conference on Robotics and Automation*, volume 2021-May, pages 7350–7356. Institute of Electrical and Electronics Engineers Inc. ISBN 978-1-72819-077-8. doi:10.1109/ICRA48506.2021.9562002.

[14] C. Folkestad, S. X. Wei, and J. W. Burdick. Quadrotor Trajectory Tracking with Learned Dynamics: Joint Koopman-based Learning of System Models and Function Dictionaries. URL http://arxiv.org/abs/2110.10341.

[15] A. Narasingam, J. Sang, and I. Kwon. Data-driven feedback stabilization of nonlinear systems: Koopman-based model predictive control. pages 1–12.

[16] SINDy with Control: A Tutorial. URL https://github.com/urban-fasel/SEIR.

[17] J. L. Proctor, S. L. Brunton, and J. Nathan Kutz. Generalizing koopman theory to allow for inputs and control. 17(1):909–930. doi:10.1137/16M1062296. URL http://www.siam.org/journals/siads/17-1/M106229.html.

[18] M. O. Williams, I. G. Kevrekidis, and C. W. Rowley. A Data–Driven Approximation of the Koopman Operator: Extending Dynamic Mode Decomposition. 25(6):1307–1346. doi:10.1007/S00332-015-9258-5/FIGURES/14. URL https://link.springer.com/article/10.1007/s00332-015-9258-5.

[19] D. C.-L. Fong and M. Saunders. LSMR: An Iterative Algorithm for Sparse Least-Squares Problems. 33(5):2950–2971. ISSN 1064-8275. doi:10.1137/10079687X. URL https://epubs.siam.org/doi/abs/10.1137/10079687X.

[20] C. C. Paige and M. A. Saunders. LSQR: An Algorithm for Sparse Linear Equations and Sparse Least Squares. 8(1):43–71. ISSN 0098-3500, 1557-7295. doi:10.1145/355984.355989. URL https://dl.acm.org/doi/10.1145/355984.355989.

[21] P. Strobach. Recursive Least-Squares Using the QR Decomposition. In P. Strobach, editor, *Linear Prediction Theory: A Mathematical Basis for Adaptive Systems*, Springer Series in Information Sciences, pages 63–101. Springer. ISBN 978-3-642-75206-3. doi:10.1007/978-3-642-75206-3_4. URL https://doi.org/10.1007/978-3-642-75206-3_4.

[22] A. Sayed and T. Kailath. *Recursive Least-Squares Adaptive Filters*, volume 20094251 of *Electrical Engineering Handbook*, pages 1–40. CRC Press. ISBN 978-1-4200-4606-9 978-1-4200-4607-6. doi:10.1201/9781420046076-c21. URL http://www.crcnetbase.com/doi/abs/10.1201/9781420046076-c21.

[23] A. Ghirnikar and S. Alexander. Stable recursive least squares filtering using an inverse QR decomposition. In *International Conference on Acoustics, Speech, and Signal Processing*, pages 1623–1626 vol.3. doi:10.1109/ICASSP.1990.115736.

[24] T. A. Howell, B. E. Jackson, and Z. Manchester. ALTRO: A Fast Solver for Constrained Trajectory Optimization. pages 7674–7679. ISSN 9781728140049. doi:10.1109/IROS40897.2019.8967788.

[25] B. E. Jackson, T. Punnoose, D. Neamati, K. Tracy, R. Jitosho, and Z. Manchester. ALTRO-C: A Fast Solver for Conic Model-Predictive Control; ALTRO-C: A Fast Solver for Conic Model-Predictive Control. ISSN 9781728190778. doi:10.1109/ICRA48506.2021.9561438. URL https://github.com/.

[26] Z. Manchester, J. Lipton, R. Wood, and S. Kuindersma. A Variable Forward-Sweep Wing Design for Enhanced Perching in Micro Aerial Vehicles. In *AIAA Aerospace Sciences Meeting*. URL https://rexlab.stanford.edu/papers/Morphing_Wing.pdf.

[27] T. A. Howell, S. Le Cleac', J. Z. Kolter, M. Schwager, and Z. Manchester. Dojo: A Differentiable Simulator for Robotics.

[28] E. Todorov, T. Erez, and Y. Tassa. MuJoCo: A physics engine for model-based control. In *2012 IEEE/RSJ International Conference on Intelligent Robots and Systems*, pages 5026–5033. doi:10.1109/IROS.2012.6386109.